

# Mechanical properties of carbon fibre-reinforced glasses

H. HEGELER\*, R. BRÜCKNER

*Institut für Nichtmetallische Werkstoffe, Anorganische Werkstoffe, Technische Universität Berlin, Englische Strasse 20, 1000 Berlin 12, Germany*

Carbon fibre-reinforced glasses exhibit very high values of flexural strength but usually a much less controlled fracture behaviour than SiC fibre-reinforced glasses. Some carbon fibre/glass composite combinations show a well controlled fracture, others a brittle fracture behaviour. The former combinations occasionally exhibit an increase in strength after an abrupt breakdown from the maximum strength. No correlation exists between the strength of the composites and the stresses in the glass matrix due to the thermal expansion mismatch between carbon fibres and glasses in contrast to the SiC fibre composites. The reason for that is seen in the structure of the surface and mainly in the anisotropic properties of the fibres, such as the large differences in the Young's moduli and thermal expansion coefficients parallel and perpendicular to the fibre axis. In particular, no radial compressive stress on the fibres can be built up at the fibre/glass interface because the thermal expansion coefficient of the fibres in the radial direction is much larger than that of the glass matrices used. Thus, the mechanism of load transfer from the matrix to the fibres is a complicated one, and cannot easily be predicted as in the case of the isotropic SiC fibres. A possible mechanism is described in order to interpret the experimental results.

## 1. Introduction

In order to improve the mechanical properties of glasses, particularly the strength, toughness, fracture strain and Young's modulus, carbon fibres are used as a reinforcement component in uni- and bi-directionally fibre-reinforced glass composites. In the present study two types of high tensile strength carbon fibres (HT-fibres) were incorporated into various glasses, which mainly differ in their thermal expansion coefficients and glass transition temperatures. Attempts were made to find a correlation between the strength of the composites and the interior stresses resulting from the thermal expansion mismatch analogous to the unidirectionally SiC fibre-reinforced glasses [1].

## 2. Experimental procedure

### 2.1. Materials

The HT carbon fibres and their properties are listed in Table I. The glasses used were the same commercial and laboratory glasses applied previously for the SiC fibre-reinforced glasses [1]: the borosilicate glass DURAN; the phosphate-containing alkaline earth alumino borosilicate glass Supremax; an alkali-poor alumino-borosilicate glass (glass D); a phosphate-free alkaline earth aluminosilicate glass (glass H); a ZrO<sub>2</sub>-containing alkali-alkaline earth silicate glass (glass B); and an alkali-poor alumino-borosilicate glass (glass A). Another glass with a very low thermal expansion

coefficient was used with the composition as powder of 97% SiO<sub>2</sub> glass and 3% DURAN glass (called SiO<sub>2</sub>). The DURAN glass was added to reduce the viscosity of pure silica glass, thus this glass corresponds to Vycor glass. The most important data for the glasses are given in Table II.

### 2.2. Preparation of the composites and methods of measurements

The preparation of the prepregs was done according to a new technique described previously [2]. The densification of these prepregs was performed in a modified manner to that in [2], in which the pressure did not act only at the working temperature,  $V_A$  (see Table II), but acted slowly from the glass transition temperature,  $T_g$ , onwards. This modification should lend additional help to the inert atmosphere to prevent oxidation of the carbon fibres.

All composites were prepared in such a way that the fibre content was constant  $42 \pm 2$  vol %.

The determination of the flexural strength and of the  $K_{IC}$  values was done with the three-point method. The support distance was chosen in such a way that the ratio of length to thickness of the samples was larger than 18 [3]. Five specimens were used for the determination of each mean value. Stress-strain curves were obtained from a servo-hydraulic test machine (MTS).

\*Present address: Didier-Werke, Wiesbaden, Germany

TABLE I Properties of the carbon fibres used (producers values)

Fibre type	Fibre diameter ( $\mu\text{m}$ )	Strength (GPa)	Fracture strain (%)	Density ( $\text{g cm}^{-3}$ )	Young's modulus (GPa)	Number of monofilaments in the bundle
T800	5.5	5.59	1.9	1.81	294	6 000
T1000	5.3	7.06	2.4	1.82	294	12 000

TABLE II Properties of the applied glasses ( $\alpha$ , thermal expansion coefficient;  $T_g$ , glass transition temperature;  $V_A$ , working temperature with  $\log \eta = 4$  ( $\eta$  in dPa s))

Glass	Young's modulus (GPa)	Density ( $\text{g cm}^{-3}$ )	$\alpha$ ( $10^{-6} \text{K}^{-1}$ ) (20–300 °C)	$T_g$ (°C)	$V_A$ (°C) at $\log \eta = 4$
DURAN	63	2.23	3.25	530	1260
SUPREMAX	90	2.56	4.10	730	1230
Glass A	73	2.44	2.09	624	1324
Glass H	81	2.63	4.60	720	1254
$\text{SiO}_2 + 3\% \text{ DURAN}$	72	2.20	0.70	1220	> 1700
Glass B	85	2.75	6.60	620	1095
Glass D	85	2.54	4.10	643	1180

### 3. Results

In order to determine the optimum pressing temperature for a constant densification pressure of 10 MPa for the combination of glasses used with the T800 fibre, the strength of the composites was determined as a function of pressing temperature (for example, see Fig. 1a and b).

The temperatures with the maximum strength values of the composites were also used for the preparation of the composites with the T1000 fibres (pressure also 10 MPa).

Examples of the stress-strain diagrams for glasses reinforced with the T800 fibres are given in Fig. 2a and b and for those reinforced with the T1000 fibres in Fig. 3a and b. The matrix glasses chosen for illustration are DURAN (Figs 2a, 3a) and SUPREMAX (Figs 2b, 3b). Tables III and IV summarize the main properties of all composites. Generally one may state that high-strength values and in most cases a relatively good toughness are obtained in comparison to the unreinforced bulk glasses. Although the tensile strength of the T1000 fibre is larger than that of the T800 fibre, the flexural strengths of the composites with T1000 fibres are not always larger than those with the T800 fibres. It is remarkable that the strain values at the bendover stress, as well as at the maximum fracture stress of the composites with the T1000 fibres, do not differ much from those of the composites with the T800 fibres, although the strain value at fracture of the pure T1000 fibre is 2.4% and that of the T800 fibre is only 1.9%.

The measured densities (examples given in Fig. 1a and b and in Tables III and IV) are lower than the calculated ones for all composites. Scanning electron micrographs show, however, a very good densification of the composites, thus, pores or unfilled space between fibres and matrix could not be observed if the optimum pressing temperature was applied for preparation. Thus, the only reason for the lower densities is that the carbon fibres shrink away from the glass

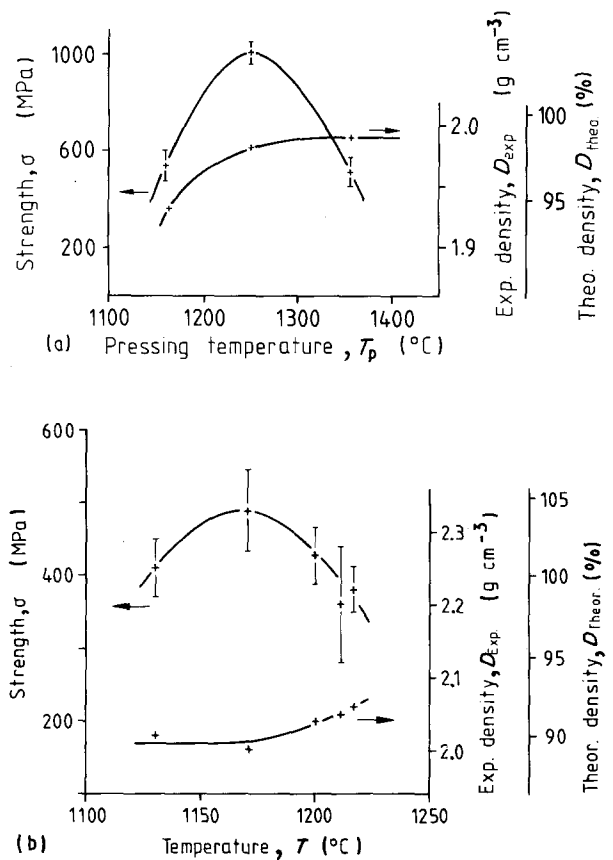


Figure 1 Flexural strength and density of carbon (T800) fibre-reinforced glass composites versus pressing temperature. Fibre content  $42 \pm 2$  vol %; pressure 10 MPa; pressing time 5 min. (a) DURAN glass; (b) SUPREMAX glass.

matrix due to the larger radial thermal expansion coefficient of the carbon fibres [4, 5] and this obviously could not be resolved directly with SEM.

### 4. Discussion

The results have shown that strength and toughness

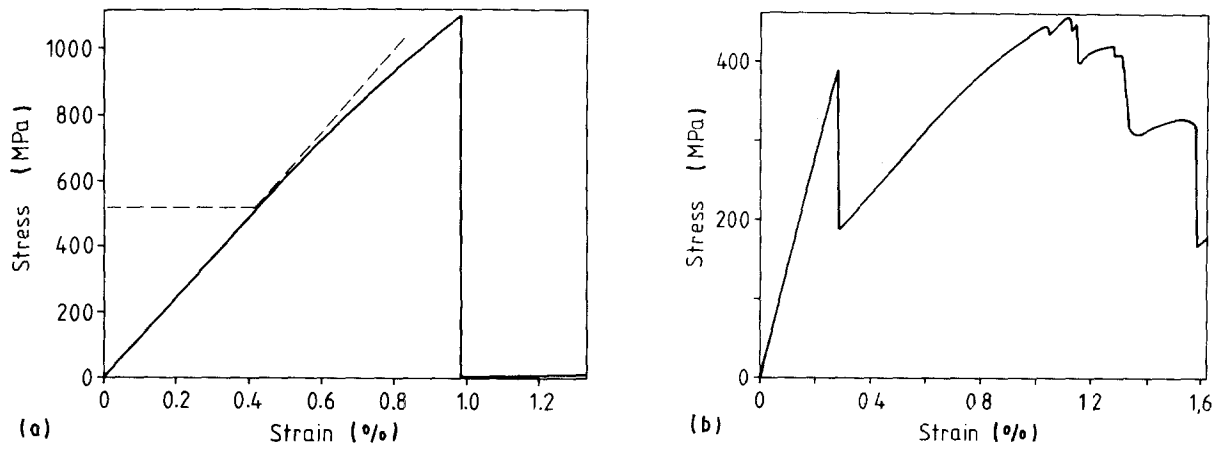


Figure 2 Stress-strain diagrams of carbon (T800) fibre-reinforced glass composites; pressure 10 MPa. (a) DURAN glass,  $T_p = 1270^\circ\text{C}$ ; (b) SUPREMAX glass,  $T_p = 1170^\circ\text{C}$ .

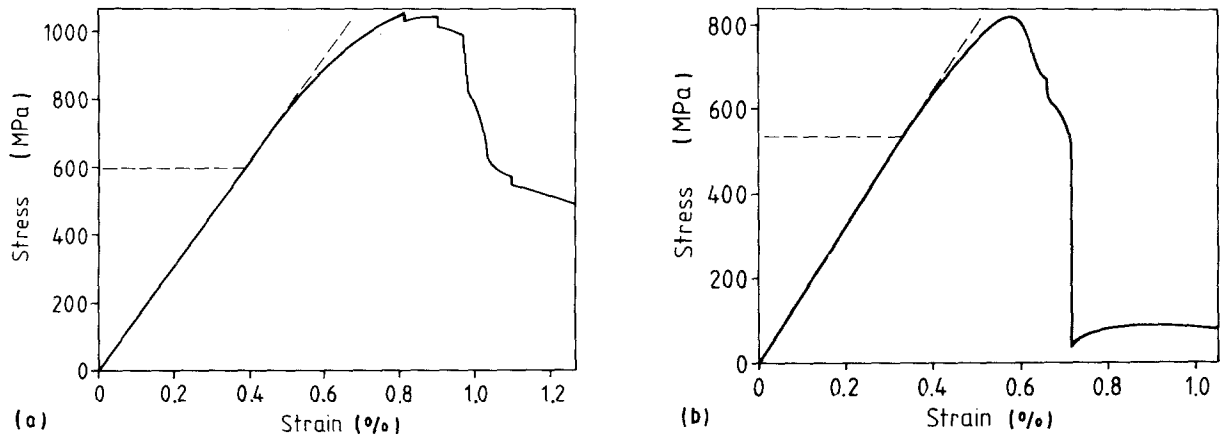


Figure 3 Stress-strain diagrams of carbon (T1000) fibre-reinforced glass composites; pressure 10 MPa. (a) DURAN glass,  $T_p = 1260^\circ\text{C}$ ; (b) SUPREMAX glass,  $T_p = 1170^\circ\text{C}$ .

TABLE III Properties of the composites glass/carbon (T800) fibre with a fibre content of  $42 \pm 2$  vol %

Glass	Strength (MPa)	Bendover stress (% strength)	$K_{IC}$ (MPa m <sup>1/2</sup> )	Young's modulus (GPa)		Density (g cm <sup>-3</sup> )		Strain (%) at	
				Exp.	Theor.	Exp.	Theor.	Bendover	Ultimate strength
SiO <sub>2</sub>	426 ± 39	-	-	178 ± 3	164	1.97	2.04	-	0.25
Glass A	934 ± 136	62	-	158 ± 9	166	2.09	2.18	0.50	1.0
DURAN	1004 ± 36	47	28 ± 3	128 ± 6	158	1.98	2.05	0.45	1.0
SUPREMAX	487 ± 56	81	-	136 ± 4	174	2.00	2.24	0.30	1.1
Glass D	1417 ± 102	38	-	147 ± 5	173	2.17	2.23	0.50	1.4
Glass H	768 ± 81	61	-	137 ± 7	169	2.07	2.28	0.3	1.5
Glass B	924 ± 58	48	-	140 ± 3	173	2.10	2.35	0.5	0.9

TABLE IV Properties of the composites glass/carbon (T1000) fibre with a fibre content of  $42 \pm 2$  vol %

Glass	Strength (MPa)	Bendover stress (% strength)	$K_{IC}$ (MPa m <sup>1/2</sup> )	Young's modulus (GPa)		Density (g cm <sup>-3</sup> )		Strain (%) at	
				Exp.	Theor.	Exp.	Theor.	Bendover	Ultimate strength
SiO <sub>2</sub>	687 ± 18	87	14 ± 2	190	165	1.92	2.04	0.3	0.35
Glass A	928 ± 92	60	29 ± 9	159	166	2.10	2.18	0.5	0.9
DURAN	1287 ± 41	62	30 ± 6	154	160	1.94	2.06	0.4	0.8
SUPREMAX	810 ± 46	68	22 ± 5	149	175	2.02	2.25	0.3	0.55
Glass D	852 ± 75	43	23 ± 1	138	173	2.08	2.23	0.28	0.87
Glass H	1148 ± 71	81	19 ± 6	167	170	1.98	2.29	0.4	0.65
Glass B	626 ± 79	41	24 ± 5	122	173	2.24	2.36	0.3	0.85

are increased drastically by the incorporation of carbon fibres into the various glass types investigated here, despite the fact that this increase is very specific and dependent on the glass type. Both properties should depend on the load-transfer mechanism from the glass matrix to the carbon fibres. While this effect was clearly determined by the degree of shrinking of the matrix on the fibres in the SiC reinforcement of the same glass types [1], this is not valid for the carbon fibre reinforcement of these glasses. One of the reasons is that the carbon fibres have no isotropic properties in contrast to the SiC fibres. The thermal expansion coefficient in the direction of the fibre axis is nearly zero, whereas perpendicular to that, the thermal expansion coefficient is  $26 \times 10^{-6} \text{ K}^{-1}$ , much larger than that of the isotropic glass matrix, and thus the carbon fibres shrink away from the matrix in the radial direction. Despite this fact, and despite the lack of theory for the calculation of stresses within composites with anisotropic fibres, the stresses within the composites produced by the thermal expansion mismatch between glass and fibres were calculated (better estimated) in the same way as previously done for isotropic SiC fibre/glass composites [1]. The applied equations are given in [1] and are based on the one-dimensional model (1) of Aveston [6], on the one hand, and on the three-dimensional model (2) of Hull and Bürger [7] on the other hand. The calculations are related to a fibre diameter of  $5.5 \mu\text{m}$  and a glass thickness of  $2 \mu\text{m}$ . Although isotropy is one of the assumptions for the models, the anisotropic thermal expansion coefficients and the anisotropic Young's moduli of the carbon fibres were used, the latter being 294 GPa in the fibre direction and 15 GPa perpendicular to that (producer's data).

The calculations were done for two cases of characteristic temperatures,  $T_x$ , at which stresses are frozen-in during cooling the composites after preparation. Case 1:  $T_x = T_g$  (glass transition temperature) and the mean expansion coefficient of the glass; Case 2:  $T_x = T_{ds}$  and the mean expansion coefficient from room temperature up to the dilatometric softening temperature,  $T_{ds}$ , of the glass. The applied data are listed in Table V ( $\parallel$  and  $\perp$  mean parallel and perpendicular to fibre axis, respectively).

The results from Model 1 listed in Table VI show that the radial stresses for the two  $T_x$  values are tensile

TABLE VI Radial stresses in the matrix at the glass/carbon fibre boundary, estimation after Model 1 assuming that adhesion is complete

Composite with matrix	Calculated radial tensile stresses (MPa)	
	Case 1	Case 2
SiO <sub>2</sub> + 3% DURAN	288	300
Glass A	138	152
DURAN	108	127
SUPREMAX	153	161
Glass D	133	156
Glass H	144	153
Glass B	113	119

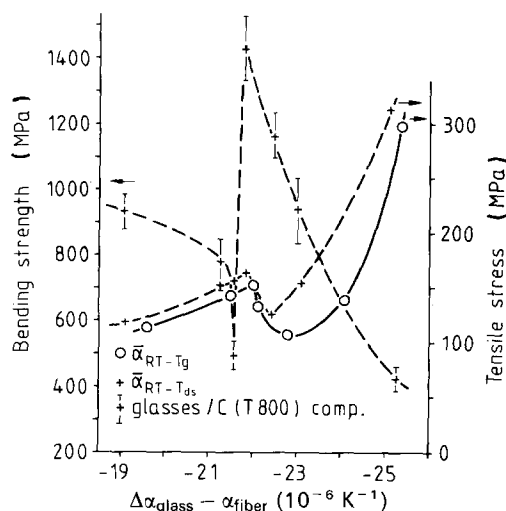


Figure 4 Measured ultimate flexural strength and calculated stresses of the matrix at the fibre/matrix boundary after Model 1 for all seven glasses reinforced with carbon (T800) fibres as a function of the differences between the thermal expansion coefficients of fibre and glasses for two cases of stress freezing-in temperatures:  $T_g$  (glass transition temperature) and  $T_{ds}$  (dilatometric softening temperature). (O)  $\bar{\alpha}_{RT} - T_g$ ; (+)  $\bar{\alpha}_{RT} - T_{ds}$ ; (+) glasses/carbon (T800) composites.

stresses as expected, and therefore no load transfer should be possible. The graphic diagram in Fig. 4 shows that the stresses are not correlated directly to the difference of the thermal expansion coefficients between carbon fibres and glasses in contrast to [1], with SiC fibres and the same glasses. The curve for the

TABLE V Thermal expansion coefficients,  $\alpha$ , of the carbon fibres and of the applied glasses. The indices  $T_g$  and  $T_{ds}$  mean that the mean values are those up to  $T_g$  (transition temperature) and  $T_{ds}$  (dilatometer softening temperature), respectively

Composite with matrix glasses	$T_{Tx}$ (°C)	$T_{ds}$ (°C)	$\alpha$ of glass ( $10^{-6} \text{ K}^{-1}$ )		$\alpha$ of fibre ( $10^{-6} \text{ K}^{-1}$ )			
			$T_g$	$T_{ds}$	$T_g$		$T_{ds}$	
					$\parallel$	$\perp$	$\parallel$	$\perp$
SiO <sub>2</sub> + 3% DURAN	1200	1290	0.60	0.90	0.15	25.97	0.15	26.00
Glass A	624	705	1.87	2.85	0.00	25.92	0.05	25.95
DURAN	530	630	3.16	3.52	-0.03	25.90	0.00	25.92
SUPREMAX	730	780	3.82	4.17	0.05	25.92	0.08	25.95
Glass D	643	720	3.79	4.38	0.00	25.92	0.07	25.95
Glass H	720	770	4.45	4.70	0.05	25.92	0.08	25.95
Glass B	620	670	6.35	6.89	0.00	25.92	0.00	25.95

radial tensile stress in Case 2 ( $T_x = T_{ds}$ ; dashed line) are shifted to lower differences of thermal expansion mismatch with respect to Case 1 ( $T_x = T_g$ ). Also the bending strength values of the composites glass/carbon fibre (T800) do not show any direct correlation to the thermal expansion mismatch. This, however, was expected qualitatively, as was mentioned above.

Similar results are obtained from Model 2 (Fig. 5a and b): tensile stresses in the radial and axial (tangential) and compressive stresses in the azimuthal direction. Also no direct correlation is found between the calculated stresses, on the one hand, and the thermal expansion mismatch (Fig. 6) and the bending strength of the composites (compare Fig. 6 and the curve for the strength in Fig. 4), on the other hand.

In addition, the toughness, which is relatively high as seen already from Figs 2 and 3 and which is also demonstrated by direct measurements of  $K_{IC}$  according to the method used for isotropic materials, does

not show a direct relationship with the thermal expansion mismatch (Fig. 7). Usually the glass/carbon fibre (T1000) composites show a better toughness than the glass/carbon fibre (T800) composites.

As a main result, there is no simple and direct correlation between the calculated stresses within the matrix at the fibre/matrix interface and the bending strength of the matrix as a function of the thermal expansion mismatch, as was the case with SiC fibre/glass composites [1]. Moreover, while the strength of the SiC fibre/glass composites is a direct function of the thermal shrinking of the glass matrix on the fibres, which leads to a load transfer from the matrix to the fibres, this simple concept is not valid or at least not the dominating concept for the carbon fibre/glass composites. The more surprising is that the carbon fibre/glass composites show relatively high bending strength values, even partly larger than those of the SiC fibre/glass composites.

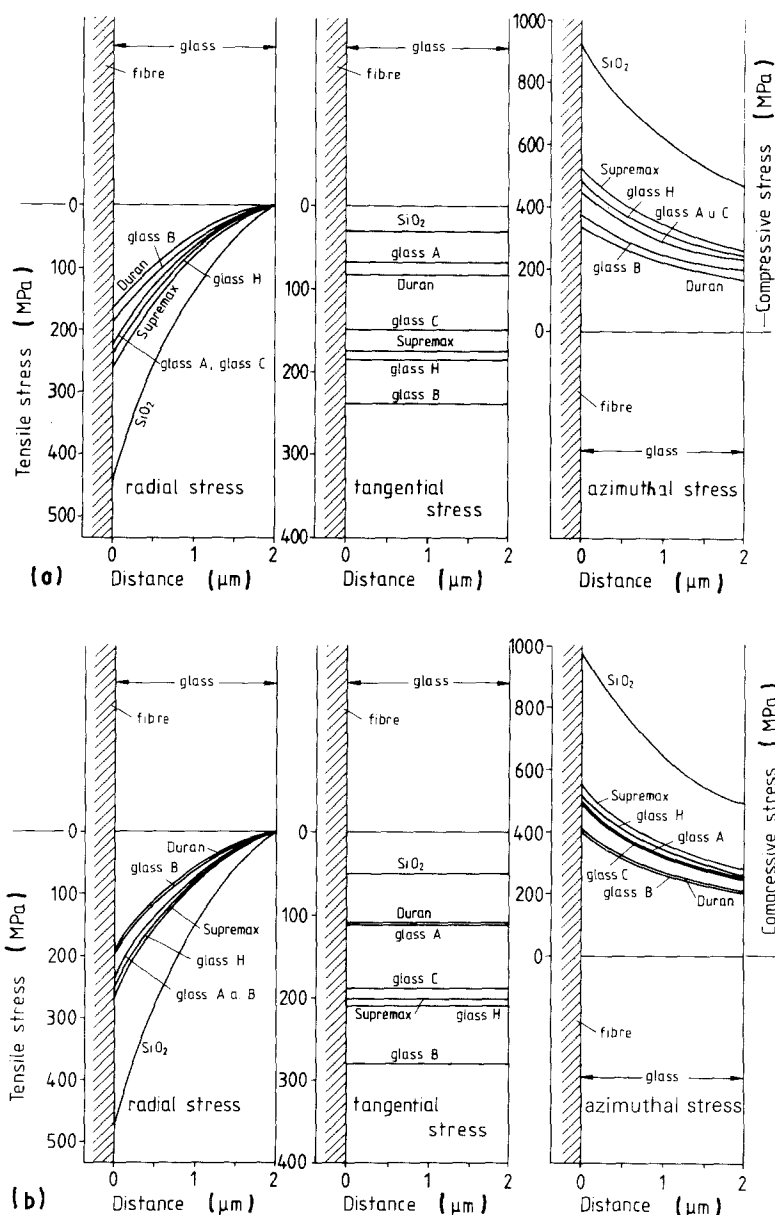


Figure 5 Stresses within the various glass matrices versus distance from the carbon (T800) fibre calculated after Model 2, for two cases of stress freezing-in temperatures, (a)  $T_g$  and (b)  $T_{ds}$  (see caption of Fig. 4).

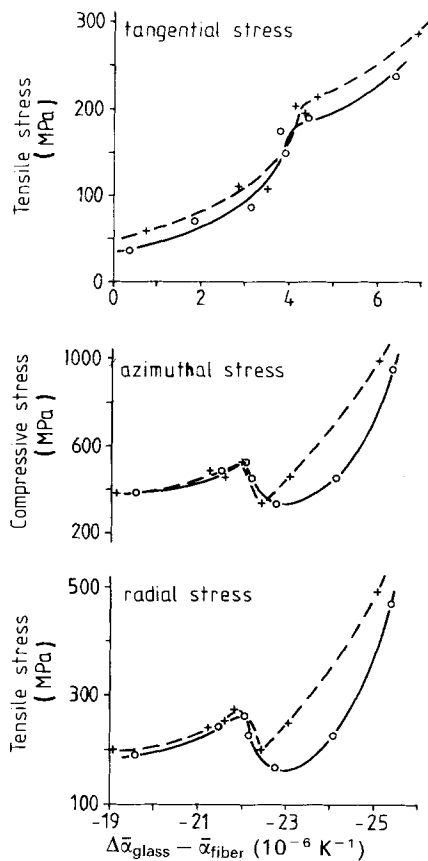


Figure 6 Calculated stress components in the matrix at the fibre/matrix boundary after Model 2 for all seven glasses reinforced with carbon (T800) fibres versus the differences between the thermal expansion coefficients of fibre and glasses for two cases of stress freezing-in temperatures:  $T_g$  and  $T_{ds}$  (see caption of Fig. 4). (○)  $\Delta\bar{\alpha}_{RT} - T_g$ , (+)  $\Delta\bar{\alpha}_{RT} - T_{ds}$ .

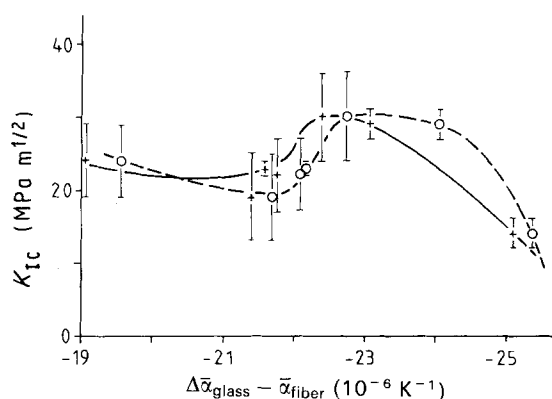


Figure 7 Toughness ( $K_{IC}$  values) of all seven glasses reinforced with carbon (T1000) fibres versus the differences of the thermal expansion coefficients of fibre and glasses for two cases of stress freezing-in temperatures:  $T_g$  and  $T_{ds}$  (see caption of Fig. 4). (○)  $\Delta\bar{\alpha}_{RT} - T_g$ , (+)  $\Delta\bar{\alpha}_{RT} - T_{ds}$ .

## 5. Conclusions

As was already argued above and confirmed by the preceding estimations, the fibres shrink away from the matrix. The question is now: do they produce really radial tensile stresses in the matrix or do they delaminate thermally on cooling after preparation by the hot-pressing procedure?

The origin of the really existing load-transfer mechanism between the carbon fibres and the glass matrix

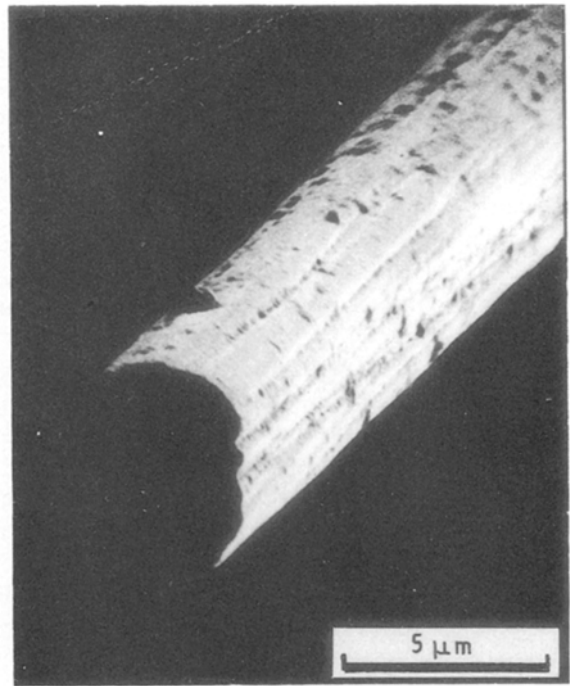


Figure 8 Scanning electron micrograph of the carbon (T800) fibre.

ces might be (i) the strongly structured surface of the carbon fibres, particularly that of the T800 fibre (Fig. 8); and (ii) the adhesion of at least part of the cylindrical surface per unit length of the fibres to the glass matrix. Otherwise the composites could not show the fracture features which are demonstrated by the results of Sections 3 and 4. The mechanical adhesion and interlocking effect may be supported by a certain degree of twisting of the fibre bundle.

The adhesion effect is demonstrated in more detail by the schematic Fig. 9a-c. The radial shrink effect of the carbon fibre does not take place in a symmetrical manner such that the fibres have no adhesive connection around the total cylindrical surface (Fig. 9a) but with a more or less contact interface to the matrix (Fig. 9b). This contact area might usually have an asymmetrical cross-section due to an asymmetrical radial thermal delamination process. In that way the contact area between fibre and matrix is larger than that of a symmetrical delamination. This kind of adhesive contact area is supported by the shrinking matrix and by the non-shrinking carbon fibre along its axis. In this way the fibres are compressed axially and are forced to contact the matrix in a screw-like and/or wavy manner, as is indicated in Fig. 9c. This model-like interpretation is confirmed by the fact that the bendover stresses of the carbon fibre-reinforced glass composites are usually lower than those of the SiC fibre-reinforced glass composites [1] despite the usually larger maximum stress, because the load transfer in the case of the SiC fibres is immediate and direct, while in the case of the carbon fibres the load transfer acts with a certain delay of strain due to the described incomplete contact area (Fig. 9b and c). Therefore, the glass matrix is more strained until the full load is transferred to the carbon fibre and the bendover

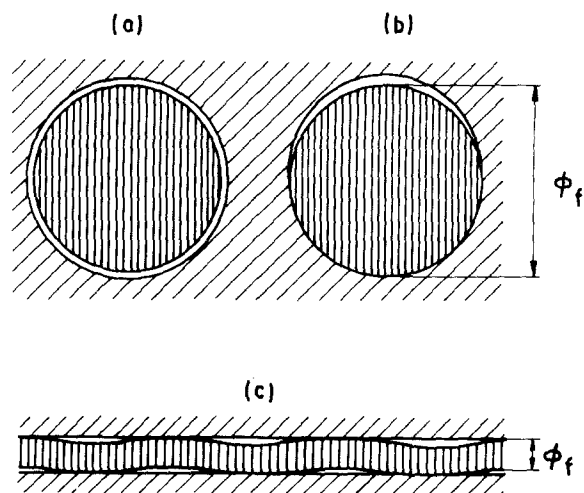


Figure 9 Schematic sketches for three situations of carbon fibre/glass matrix adhesions: (a) total radial delamination of the carbon fibre from the glass matrix by the radial thermal expansion mismatch; (b) partial radial delamination or partial adhesion, respectively; and (c) forced adhesion by axial thermal expansion mismatch between carbon fibre and glass matrix.

stresses are lower in the latter (carbon fibre/glass composites) than in the former case (SiC fibre/glass composites). In other words: the pull-out effect starts in the case of glass/SiC fibre composites with the full friction stress between fibre and matrix; in the case of glass/carbon fibre composites, the pull-out effect starts with an elongation effect of the wavy carbon fibre (Fig. 9c) and continues with a reduced friction stress due to the incomplete contact area.

This interpretation considers, of course, only the overall main phenomena with respect to maximum stress and bendover stress. In detail there has to be considered additionally the interface condition. One hint in this direction is the surface structure of the fibres. The surface of the carbon (T1000) fibre is much smoother than that of the carbon (T800) fibre which

has led to a somewhat better fracture toughness. A second hint is that for the very smooth surface of the SiC fibres, a gliding layer of carbon plays an important role in the toughness of the SiC fibre glass composites [1, 9–11].

### Acknowledgements

The authors are grateful to the Bundesministerium für Forschung und Technologie (BMFT), Bonn, for financial support and to the SCHOTT Glaswerke, Mainz, and particularly to Dr W. Pannhorst and Dr M. Spallek, for supplying the glasses and for discussions. The contract with BMFT was under no. 03 M 10350. Responsibility for results and text belongs to the author.

### References

1. H. HEGELER and R. BRÜCKNER, *J. Mater. Sci.* **25** (1990) 4836.
2. *Idem.*, *ibid.* **24** (1989) 1191.
3. A. W. CHRISTIANSEN, J. B. LILLY and J. B. SHORTALL, *Fibre Sci. Technol.* **7** (1974) 1.
4. F. ENTWISLE, *Phys. Lett.* **2** (1962) 236.
5. J. B. NELSON and D. P. RILEY, *Phys. Soc. Proc.* **57** (1945) 477.
6. J. AVESTON, in "Strength and Toughness in Fibre-Reinforced Ceramics", Conference Proceedings (National Physical Laboratory Teddington, 1972) pp. 63–73.
7. A. W. HULL and E. E. BÜRGER, *Phys.* **5** (1934) 384.
8. K. F. ROGERS, L. N. PHILLIPS and D. M. KINGSTON-LEE, *J. Mater. Sci.* **12** (1977) 718.
9. J. J. BRENNAN, *Mater. Sci. Res.* **21** (1987) 387.
10. B. MEIER and G. GRATHWOHL, *Fresenius Z. Anal. Chem.* **333** (1989) 388.
11. W. PANNHORST, M. SPALLEK, R. BRÜCKNER, H. HEGELER, C. REICH, G. GRATHWOHL, B. MEIER and D. SPELMANN, *Ceram. Engng Sci. Proc.* **11** (1990) 947.

Received 4 December 1990  
and accepted 13 May 1991